FULL PAPER

BJC

British Journal of Cancer (2016) 115, 920–928 | doi: 10.1038/bjc.2016.263

Keywords: tyrosine kinase inhibitor; resistance; MEK inhibitor; renal cell carcinoma; myeloid-derived suppressor cell; transcriptome

MEK inhibition abrogates sunitinib resistance in a renal cell carcinoma patient-derived xenograft model

C Marcela Diaz-Montero[1,8], Frances J Mao[1,2,8], John Barnard[3], Yvonne Parker[4], Maryam Zamanian-Daryoush[5], John J Pink[6], James H Finke[1], Brian I Rini[7] and Daniel J Lindner*[,4]

[1]Department of Immunology, Lerner Research Institute, Cleveland Clinic, 9500 Euclid Avenue R40, Cleveland, OH 44195, USA; [2]Cleveland Clinic Lerner College of Medicine, Cleveland Clinic, 9500 Euclid Avenue R40, Cleveland, OH 44195, USA; [3]Quantitative Health Sciences Department, Cleveland Clinic, 9500 Euclid Avenue R40, Cleveland, OH 44195, USA; [4]Department of Translational Hematology and Oncology Research, Cleveland Clinic Taussig Cancer Institute, Cleveland Clinic, 9500 Euclid Avenue R40, Cleveland, OH 44195, USA; [5]Department of Cellular and Molecular Medicine and Center for Cardiovascular Diagnostics and Prevention, Cleveland Clinic, 9500 Euclid Avenue R40, Cleveland, OH 44195, USA; [6]Case Comprehensive Cancer Center, Case Western Reserve University Medical School, Cleveland Clinic, 9500 Euclid Avenue R40, Cleveland, OH 44195, USA and [7]Department of Solid Tumor Oncology, Cleveland Clinic Taussig Cancer Institute, Cleveland Clinic, 9500 Euclid Avenue R40, Cleveland, OH 44195, USA

Background: Renal cell carcinoma (RCC) patients treated with tyrosine kinase inhibitors (TKI) typically respond initially, but usually develop resistance to therapy. We utilised transcriptome analysis to identify gene expression changes during development of sunitinib resistance in a RCC patient-derived xenograft (PDX) model.

Methods: RCC tumours were harvested during pre-treatment, response and escape phases. Direct anti-proliferative effects of sunitinib plus MEK inhibitor were assessed. Activation status (phosphorylation) of MEK1/2 and ERK1/2 was determined, myeloid-derived suppressor cells (MDSC) sub-fractions were quantitated and G-CSF was measured by ELISA.

Results: During the response phase, tumours exhibited 91% reduction in volume, characterised by decreased expression of cell survival genes. After 4-week treatment, tumours developed resistance to sunitinib, associated with increased expression of pro-angiogenic and cell survival genes. During tumour escape, cellular movement, inflammatory response and immune cell trafficking genes were induced, along with intra-tumoural accumulation of MDSC. In this PDX model, either continuous treatment with sunitinib plus MEK inhibitor PD-0325901, or switching from sunitinib to PD-0325901 was effective. The combination of PD-0325901 with TKI suppressed intra-tumoural phospho-MEK1/2, phospho-ERK1/2 and MDSC.

Conclusions: Continuous treatment with sunitinib alone did not maintain anti-tumour response; addition of MEK inhibitor abrogated resistance, leading to improved anti-tumour efficacy.

Vascular endothelial growth factor (VEGF) receptor tyrosine kinase inhibitors (TKI) are the standard of care in treating metastatic renal cell carcinoma (mRCC). However, the development of resistance to VEGF receptor inhibitors is a critical clinical management problem. Salvage therapy with another VEGF TKI or an mTOR inhibitor rarely results in durable responses, and median progression-free survival with second-line targeted therapy is generally 4–6 months (Oudard and Elaidi, 2012).

*Correspondence: Dr DJ Lindner; E-mail: lindned@ccf.org
[8]These authors contributed equally to this work.

Revised 6 July 2016; accepted 26 July 2016; published online 25 August 2016

To maximise the clinical efficacy, there is a need for better understanding of mechanisms by which mRCC evolves to escape treatment by anti-angiogenic therapy. Preclinical studies suggest that upregulation of angiogenic proteins (angiopoietin, IL-8, PIGF and FGF) leading to VEGF-independent angiogenesis may drive tumour growth during continuous VEGF signal suppression (Casanovas *et al*, 2005; Fischer *et al*, 2007; Huang *et al*, 2010b). More specifically, FGFs (Welti *et al*, 2011) and HGF (Shojaei *et al*, 2010) have been shown to mediate sunitinib resistance. Patients with advanced RCC that develop resistance to VEGF inhibition display upregulation of IL-6 as well as bFGF and HCF, all of which are angiogenic (Porta *et al*, 2013).

Myeloid-derived suppressor cells (MDSC), have been implicated in the resistance to anti-angiogenic therapy. Tumour infiltration by CD11b + Gr1 + MDSC conferred resistance to bevacizumab (anti-VEGFA antibody) (Shojaei *et al*, 2007a). The endocrine-derived VEGF homologue Bv8 promotes mobilisation of MDSC from the bone marrow (Shojaei *et al*, 2007b), and G-CSF is a key mediator of this mobilisation (Shojaei *et al*, 2009). G-CSF leads to activation of the RAS/MEK/ERK pathway and the Ets transcription factor (Phan *et al*, 2013). We have previously noted that MDSC had a role in development of resistance to sunitinib in RCC patients receiving anti-angiogenic therapy (Finke *et al*, 2011).

To identify potential signalling pathways utilised by tumours to circumvent anti-angiogenic therapy, a patient-derived xenograft (PDX) model of RCC was established and expression microarray analysis of sunitinib-responsive and sunitinib-resistant tumours was performed. Several MEK/MAPK-related proteins were upregulated in the TKI-resistant tumours, and a pharmacological inhibitor of this pathway-abrogated TKI resistance.

MATERIALS AND METHODS

Cell viability assay. The fraction of viable cells was determined on cells in culture using a luminescence based assay (CellTiter-Glo, Promega, Madison, WI, USA). Ren-01 and Ren-02 human RCC cells were plated in 96-well plates (10 000 cells/0.2 ml DMEM medium), allowed to adhere, and compounds (both from Pfizer, New York, NY, USA) were added. After 48 h, viability was determined using a multi-label counter (Victor^2 1420 Wallac, Perkin-Elmer, Waltham, MA, USA). Chou-Talalay analysis was used to determine whether combination drug effects were antagonistic, additive or synergistic (Chou and Talalay, 1984).

Xenograft model of renal cell carcinoma. Animal studies were approved by the Cleveland Clinic IACUC. The Ren-02 cell line was established from a patient-derived primary clear cell RCC tumour. This 42-year-old male patient had metastatic clear cell RCC with disease progression after bevacizumab therapy. A subcutaneous tumour nodule was biopsied, dissociated using the GentleMACS system (Miltenyi) and a continuous cell line established. For PDX establishment, cells were expanded *in vitro* and each of the four 6-week-old male NOD-scid-IL2r$^{-/-}$ (NSG) mice (Jackson Laboratories) were inoculated subcutaneously in the dorsal midline with 2×10^6 Ren-02 cells (passage 3) at three separate sites, 10 mm apart. For Ren-02 cells, the doubling time is ~72 h *in vitro* and ~14d *in vivo*. Ren-01 RCC PDX model and cell line was established in a similar fashion from another Cleveland Clinic patient. Both Ren-01 and Ren-02 RCC PDX retained a clear cell histology in harvested tumours (Figure 1A and B).

Each of the four mice in this study harboured three separate tumours that were harvested at three different time points under general anaesthesia. Bupivacaine was injected around the skin incision for pain relief. An incision was made over the tumour, just long enough to dissect the tumour free. Skin was sutured, and mice were allowed to recover. Time points of harvest were: 1) pre-treatment (Pre-Rx or T0), 2) at point of maximal response (Response or T1) and 3) at point of resistance (Escape or T2), thus each mouse served as its own control. A strong correlation of induced genes between animals within each time point group was reflected in tight clustering on sample relation maps.

***In vivo* drug treatment.** All drugs were administered via oral gavage (p.o.). Treatment with sunitinib 40 mg/kg/d (Pfizer) was started 14d after tumour inoculation. Axitinib (Pfizer) 30 mg/kg b.i.d. and pazopanib (GSK) 100 mg/kg b.i.d. were also utilised. MEK inhibitor PD-325901 (Pfizer) at 4 mg/kg/d was used in combination experiments. Vehicle for all compounds was 2% (w/v) carboxymethylcellulose in water. Tumour response was measured by serial caliper tumour measurements, and tumour volume (prolate spheroid) was calculated using the formula $v = 4/3\pi a^2 b$ where a = minor radius, b = major radius. Single agent and combination treatment were well tolerated *in vivo*, without evidence of weight loss. One-way ANOVA was used for statistical analysis of tumour volume between treatment groups.

qRT-PCR. RNA samples extracted from four individual tumours were used as biological replicates for qRT-PCR analyses. Each biological replicate had three technical replicates. For each sample, reverse transcription was performed on 2 μg total RNA by 200U M-MLV transcriptase (Takara). The reaction was carried out at 70 °C for 10 min, 42 °C for 60 min and 70 °C for 15 min. Resulting cDNA was diluted to 800 μl with sterile water. qPCR was carried out in triplicate using an ABI 7500 Fast instrument (Applied Biosystems/Life Technologies). Gene-specific primers were designed using PrimerQuest (Integrated DNA Technologies). The actin gene (Accession no.: ADK11998) was used as an endogenous control. PCR was carried out in 20 μl volume containing 2 μl cDNA, 250 nM forward primer, 250 nM reverse primer, and 1 × SYBR Premix Ex Taq II (TaKaRa) using the following conditions: 95 °C for 3 min, 40 cycles of 95 °C for 15 s, 60 °C for 15 s, and 72 °C for 15 s. Melting curve analyses were performed to verify the specificity by ABI 7500 Fast instrument Manage software. Relative expression levels were calculated using the $2^{-\Delta\Delta Ct}$ method (Schefe *et al*, 2006). A two group *t*-test was used for statistical analysis.

Gene array analysis. Total RNA from individual tumours was prepared using the RNeasy Mini kit (Qiagen) with on-column DNase treatment (Qiagen # 79254) per manufacturer's protocol. RNA was quantified by Nanodrop (ND-1000, Thermo Fisher Scientific) and RNA integrity was assessed by agarose gel electrophoresis. Three hundred nanograms of RNA was amplified and biotinylated for hybridisation to Illumina Human Beadchips (HumanHT-12 v.4, Illumina) and also to Murine Beadchips (mouseRef-8 v1.1) using Illumina TotalPrep RNA Amplification Kit (AMIL1791, Applied Biosystem) according to the manufacturer's protocol. After hybridisation and staining, the arrays were scanned in an Illumina Bead Station, and the images processed using Illumina Genome Studio software (v2011.1). Probe-level data were exported for processing in R. Probes were annotated using the R packages illuminaHumanv4 and illuminaMousev2. Probe data was background adjusted using a normal-gamma deconvolution method from the R package NormalGamma, ln-transformed with an offset of 32, and then quantile normalised using the R package beadarray. Probes were removed from analyses based on detection counts, probe variation and probe quality. MDS plots were used to filter samples with aberrant expression profiles. Replicate expression data were averaged to produce one expression profile per tumour. Filtered probes were averaged per mapped gene to get a single expression measure per gene per sample. Complete microarray data was uploaded to Gene Expression Omnibus (GEO, accession number GSE76068).

Statistical analysis. Filtered expression profiles (sample relations) were visualised using multidimensional scaling. Differential expression (DE) analyses, at both the probe and gene levels, were

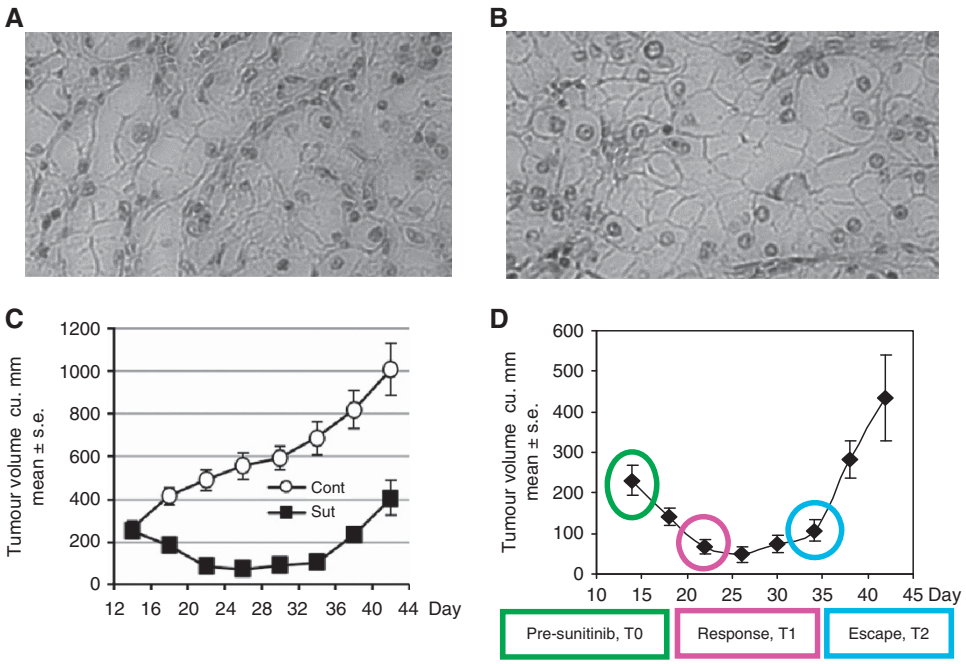

Figure 1. (**A**) Ren-01 and (**B**) Ren-02 subcutaneous PDX tumours (mice were vehicle-treated) retain clear cell phenotype of primary RCC (H&E staining, × 160). Response of Ren-02 human RCC xenograft to sunitinib and development of resistance. (**C**) Initiation of sunitinib (40 mg kg^{-1} p.o.) on d14 resulted in reduction of tumour volume (response) followed by sunitinib resistance (escape) after d30 despite continuous therapy; $P = 0.0048$. (**D**) Tumours were harvested on d14, d21 and d34 for gene expression analysis.

done using a linear model approach as implemented in the R package limma. Mouse was treated as a blocking factor accounting for within mouse correlation in the human expression analyses. Time contrasts of interest were estimated from the fitted linear models. False-discovery rates were used to control for multiple testing. Pathway analyses of the gene-level DE results were done using Ingenuity Pathway Analysis (Qiagen). A FDR threshold of 0.10 was used to select DE genes of interest in the pathway analyses.

Immunoblot analysis. RCC tumours were harvested on d62 from mice receiving daily oral drug treatment (sunitinib 40 mg/kg/d, axitinib 30 mg/kg/bid, pazopanib 100 mg/kg/bid, either as single agents or combined with PD-325901, 4 mg/kg/d). Without culturing *in vitro*, tumours were immediately lysed in cold RIPA buffer plus phosphatase inhibitors using sonication × 15 s on ice. Ren-01 cells (2×10^6) were plated in RPMI-1640 (10% FBS) in 6-well plates. Sixteen hr later cells were treated for 24 h with sunitinib (2 μM), axitinib (2 μM), or pazopanib (2 μM), either alone or in combination with PD-325901 (1 nM). Cells were washed × 2 with cold PBS and lysed in cold RIPA buffer containing phosphatase inhibitor cocktail (Sigma). Protein concentration was determined using BCA protein assay (Pierce Biotechnology). Twenty micrograms of protein were separated under reducing conditions on 4–15% gradient SDS-PAGE gels. Blots were probed with primary antibodies (anti-MEK, anti-phospho-MEK, anti-ERK, anti-phospho-ERK, from Santa Cruz Biotechnology) followed by enhanced chemiluminescence reagent (Amersham).

MDSC analysis. Phenotyping of MDSC was performed on fresh tumour samples. Tumours from each mouse were cut into 1 mm fragments, incubation (15 min) with enzyme cocktail (Sigma, Collagenase 1 mg/ml, DNase 0.1 mg/ml, hyaluronidase 2.5 U/ml) then filtered using 70 μm strainers (BD Falcon). Single cell suspension was subjected to 30–70% percoll (GE Healthcare) gradient to enrich for mononuclear cells and remove debris. Cells were counted followed by staining with anti-CD11b PE (eBioscience), anti-Ly6G FITC (BD Biosciences), and anti-Ly6C APC (BioRad) antibodies for flow cytometry (BD FACSCalibur) and analysis (FlowJo, Treestar). Differences in cell number between treatment groups were compared by *t*-test ($n = 4$).

G-CSF ELISA. Samples were divided and a portion of the tumour was flash frozen to make lysates using the Fastprep-24 (MP Biomedicals) according to the manufacturer's manual. Tumour tissue was placed in Lysing Matrix D tubes with RIPA Buffer (Thermo Scientific) and Protease inhibitor (Sigma) and Halt Phosphatase inhibitors (Thermo Scientific), incubated and processed in the FastPrep-24. Protein concentration was measured using Pierce BCA Protein Assay and the same quantity of protein was used for ELISA assays for both mouse & human G-CSF (R & D Systems). Differences in cytokine concentration between treatment groups were compared by *t*-test ($n = 4$).

RESULTS

Xenograft model of acquired TKI resistance. Human primary Ren-02 RCC cells were expanded in culture and inoculated subcutaneously into NSG mice ($n = 6$ per group, one tumour/mouse) (Jackson Laboratory) and treated with sunitinib (40 mg/kg/d p.o. d14-d42). In the sunitinib-treated group, tumours reached a nadir in size by d26, and tumour volume was decreased in the sunitinib-treated *vs* control group (48 *vs* 529.5 mm^3, $P = 0.0003$), a 91% reduction in volume (Figure 1C). This period of tumour sensitivity to drug treatment was termed the 'response' phase. Despite continuous treatment, tumours failed to maintain response to therapy post d30. Tumour regrowth in the sunitinib-treated group approached the same growth rate as untreated mice, but tumour volume was significantly less compared with the vehicle group (433.5 *vs* 1066 mm^3, $P = 0.0048$). This period of tumour resistance to drug treatment was termed the 'escape' phase. Of note, sunitinib-treated tumours at the end of the escape phase still remained ~2.5-fold smaller than mice receiving vehicle only ($P = 0.0048$). This response and subsequent resistance (Figure 1D)

is similar to that observed clinically in metastatic RCC patients (Vasudev *et al*, 2013).

Expression of mediators involved in immune cell trafficking and inflammatory response increased during escape phase. Illumina microarray analyses of RNA isolated from tumours harvested at the pre-treatment, response, and escape time points were performed. Out of the 18 320 filtered human probes analysed, which mapped to 13 396 genes, 1273 genes (1643 probes) were upregulated and 1235 genes (1663 probes) were downregulated in the tumour during escape phase compared with the response phase (raw *P*-values <0.05). Of these, 438 genes (574 probes) were significantly upregulated and 407 genes (580 probes) were significantly downregulated (FDR <0.05). Since xenografts are composed of human parenchymal and murine stromal components, the same RNA was analysed using murine probes in an attempt to elucidate the contribution of host factors to sunitinib resistance. Out of the 13 475 filtered murine probes assayed by microarray, which mapped to 10 065 genes, 455 genes (611 probes) were upregulated and 600 genes (760 probes) were downregulated in the tumour during the response phase *vs* in the pre-treatment tumour. A similar analysis found that 776 genes (955 probes) were upregulated and 1050 genes (1387 probes) were downregulated in the tumour during the resistant phase *vs* in the response phase (raw *P*-value of <0.05). Ingenuity Pathway Analysis visualisation of changes in gene expression during tumour, and during the escape phase revealed differences in dominant cell signalling pathways (Supplementary Figure 1). Resistance to sunitinib was associated with a upregulation of genes involved in cell movement and immune cell trafficking in both human and murine expression analyses. Upregulation of genes associated with inflammatory responses was more pronounced in murine than human components, whereas expression of cell survival genes was dramatically upregulated in human cells. Both human and murine immune trafficking genes were downregulated during tumour response; many of these same genes were later upregulated during escape (Table 1). These results are in agreement with other studies, in which tumour-derived factors promote the infiltration of non-tumour cell types that support the survival and growth of cancer cells (Beider *et al*, 2014; Cheah *et al*, 2015; Zhou *et al*, 2016). In the NSG model, tumour infiltrate is most likely of myeloid origin (neutrophils and monocytes) given the lack of B, T and NK cells in the host (Shultz *et al*, 2005). Our results suggest that this myeloid infiltrate induces a localised inflammatory response that contributes to angiogenesis, tumour progression and acquisition of sunitinib resistance.

MEK inhibition as a strategy to circumvent TKI resistance. Resistance to TKI treatment is an important clinical problem, and targeting a pathway involved in processes associated with sunitinib resistance, such as the MAP/ERK pathway, could represent a method to circumvent resistance. Using qRT-PCR we analysed expression of selected genes known to be affected by sunitinib treatment, or that had an association with MAP/ERK (Figure 3A). Genes involved in angiogenesis, IL-8, angiopoietin 2 (ANGPT2, expressed at sites of vascular remodelling), erythropoietin (EPO, induced by hypoxia) were upregulated during the escape phase. We observed a slight induction (<0.5-fold increase) of MEK1 and ERK1, whereas MAPKBP1 and MAPK7 were substantially induced (greater than two-fold) during the escape phase. Heat maps also suggested that development of TKI resistance was a pro-angiogenic process. Message coding for VEGFA/B (both angiogenic, both activate MAPK), CXCR4 and CXCR7 (ligation of either receptor leads to MAPK activation), EPO (confirmed induction by qRT-PCR) were upregulated during escape phase (Figure 2). Because the MEK/ERK pathway lies downstream of VEGFR, we assessed the impact of MEK inhibition on TKI resistance. We treated Ren-02 tumour-bearing mice with either sunitinib alone or in combination with PD-0325901 at different time points during TKI treatment. PD-0325901 is a synthetic, orally bioavailable MEK inhibitor (MEKi) that selectively inhibits MEK1 and MEK2 *in vivo*. Tumours in the sunitinib group were initially sensitive to treatment with maximal response being achieved by d30. After that, tumour began to grow, consistent with developing resistance. The addition of PD-0325901 at d30 resulted in a 51.3% reduction of tumour volume by the end of the study ($P=0.0054$). The most effective regimens were either continuous treatment with both drugs or switching from sunitinib to PD-0325901 monotherapy at d30, both of which reduced tumour volume by 78.6% ($P=0.0241$) and 88.5% ($P=0.0068$), respectively (Figure 3B). These data suggest that addition of a MEKi abrogated resistance to TKI treatment.

Inhibition of MEK1/2 phosphorylation by PD-0325901 restores sensitivity to TKI treatment. The impact of TKI monotherapy and/or TKI/MEKi combination therapy on phosphorylation (activation) of MEK1/2, and ERK1/2 was determined in lysates from RCC xenografts harvested on d62. A reduction in the phosphorylation of MEK1/2 and ERK1/2 was seen after monotherapy with sunitinib, axitinib, pazopanib or PD-0325901, and MEK1/2 activation was further reduced after combination TKI/MEKi therapy (Figure 4A) To rule out the possibility of this effect being intrinsic to Ren-02 tumours, and to eliminate contributions of host stromal components, we determined whether the same effect was observed in a different primary human RCC cell line (Ren-01). As observed in Ren-02 tumours, TKI monotherapy reduced MEK1/2 and ERK1/2 in Ren-01 cells two–three-fold, and this reduction was more pronounced after TKI/MEKi treatment (Figure 4B). These results suggest that the MEK1/2–ERK1/2 pathways likely contribute to sunitinib resistance, and that inhibition by use of PD-0325901 can restore sensitivity.

Sunitinib and PD-0325901 cell viability effects *in vitro*. To examine direct effects of sunitinib and PD-0325901 on RCC cells *in vitro*, cell viability assays were performed using single agents and in combination. The sunitinib IC50 values were 9 and 15 μM for Ren-01 and Ren-02, respectively (Figure 4C and D). These concentrations are $\sim 100\times$ higher than the pharmacologically relevant concentrations (0.1 μM) that inhibit receptor tyrosine kinases (Huang *et al*, 2010a). It is possible that a typical murine dosing regimen for PD-0325901 (1–4 mg kg^{-1}) can result in peak serum levels of 1–2 μM (Jousma *et al*, 2015) and therefore contribute to a direct anti-proliferative effect. However, the sunitinib regimen (20–40 mg kg^{-1}) results in serum levels that fall below 2 μM in 2 h, and display elimination half-life of 5 h (Zhou and Gallo, 2010). These findings suggest that the *in vivo* anti-tumour effect is not mediated by direct anti-proliferative drug effects on the tumour cells.

Resistance to sunitinib is associated with tumour-infiltrating myeloid-derived suppressor cells (MDSC) which are reduced by MEK inhibition. Since immune cell trafficking and inflammation-associated genes were upregulated during the escape phase

Table 1. Changes in immune trafficking gene expression

	Response	Escape
Human	↓ GM-CSF (CSF2), IL-8, IL-6, CCL2, CXCL5	↑ CCL2, CCL5, CXCL5, CXCL10
Murine	↓ CCL2, CCL4, CCL5, CXCL13	↑ CCL2, CCL4, CCL5, CXCL10, CXCL16

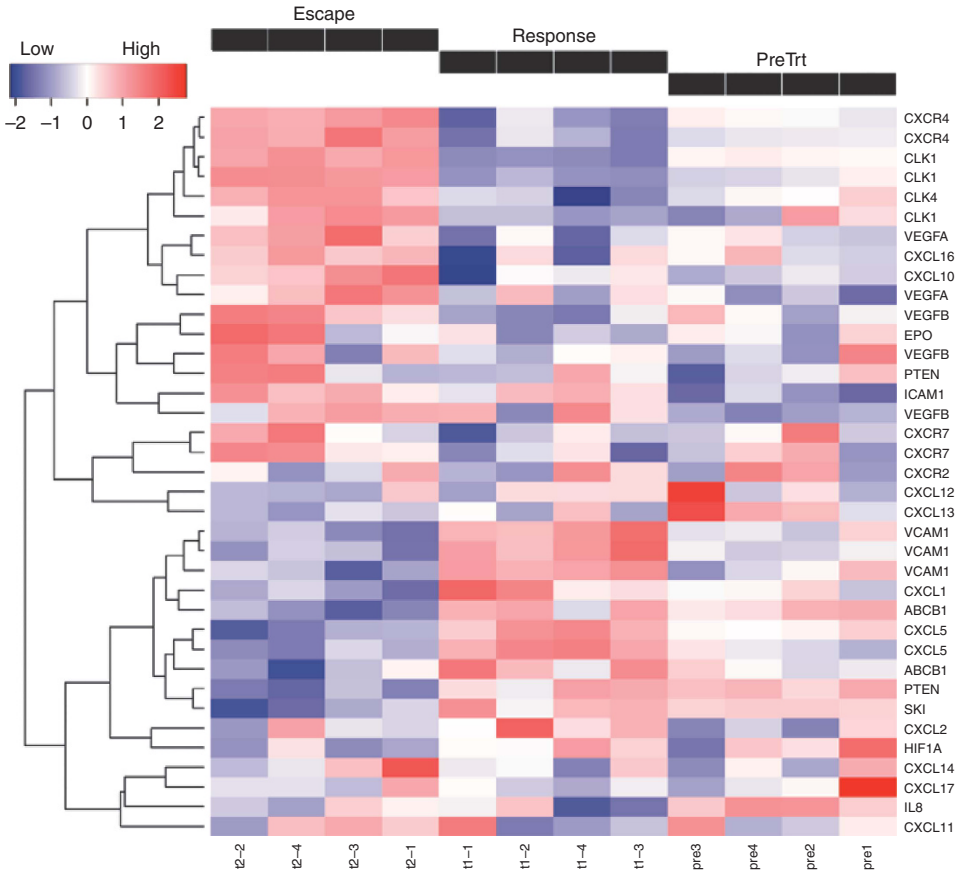

Figure 2. Hierarchical clustering and heat map analysis: Expression levels of mRNAs encoding selected human genes during escape, response and pre-treatment phase. Each column represents one individual tumour.

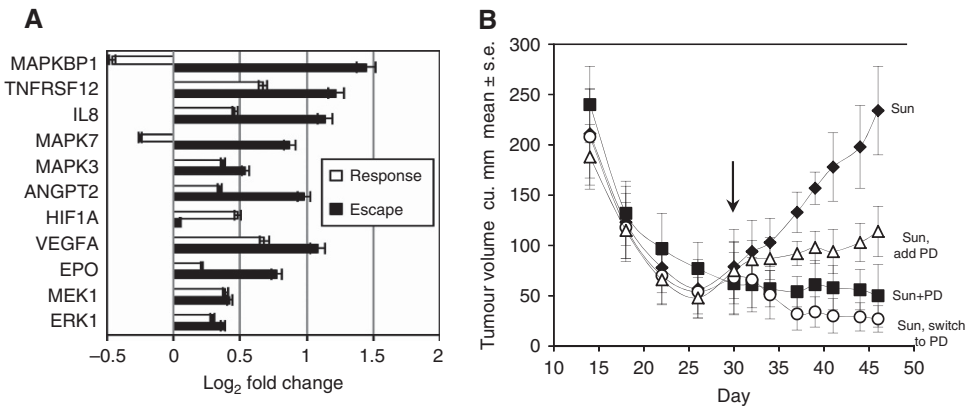

Figure 3. (A) qRT-PCR performed on tumour mRNA indicated greater than two-fold induction of VEGF-related transcripts during response phase (T1 *vs* pre) (white bars). During escape phase (T2 *vs* T1) (black bars) several pro-angiogenic transcripts were induced greater than two-fold. All changes in expression levels between response and escape phases were significant ($n=4$, $P<0.01$, *t*-test) except MEK1 and ERK1 ($P>0.05$). (**B**) Combination treatment of mice bearing Ren-02 tumours with continuous sunitinib (40 mg kg^{-1} day^{-1}) (□), continuous sunitinib + continuous MEK inhibitor (PD-325901) (4 mg kg^{-1} day^{-1}) (■), MEK inhibitor added to sunitinib on d30 (△), or sunitinib switched to MEK inhibitor on d30 (○). Tumour growth was reduced with the addition of a MEK inhibitor on d30 ($P=0.0054$), and even further reduced by continuous MEK inhibitor therapy ($P=0.0241$) or switching to MEK inhibitor monotherapy on d30 ($P=0.0068$). Continuous combination treatment (■) was not statistically different from switching from sunitinib to MEK inhibitor (○) ($P=0.076$).

(Supplementary Figure 1), and the host infiltrate in NSG mice is preferentially myeloid, we determined the role of intra-tumoural MDSC on restoration of TKI sensitivity by MEK inhibition. MDSC are classified as M-MDSC or G-MDSC according to their phenotypic and functional similarities to monocytes or granulocytes, respectively. Both M-MDSC and G-MDSC can exert immunosuppressive activity via T- and NK-cell inhibition, whereas G-MDSC can also promote angiogenesis and tumour metastasis (Kumar *et al*, 2016). G-MDSC may be more effective at impairing proliferation of T cells compared with M-MDSC (Raber *et al*, 2014). We and others have reported that in RCC patients, G-MDSC are the predominant subtype (Ko *et al*, 2009). Consistent with this, the frequency of M-MDSC in Ren-02 tumours was very low, and thus minimally affected by treatment. In contrast,

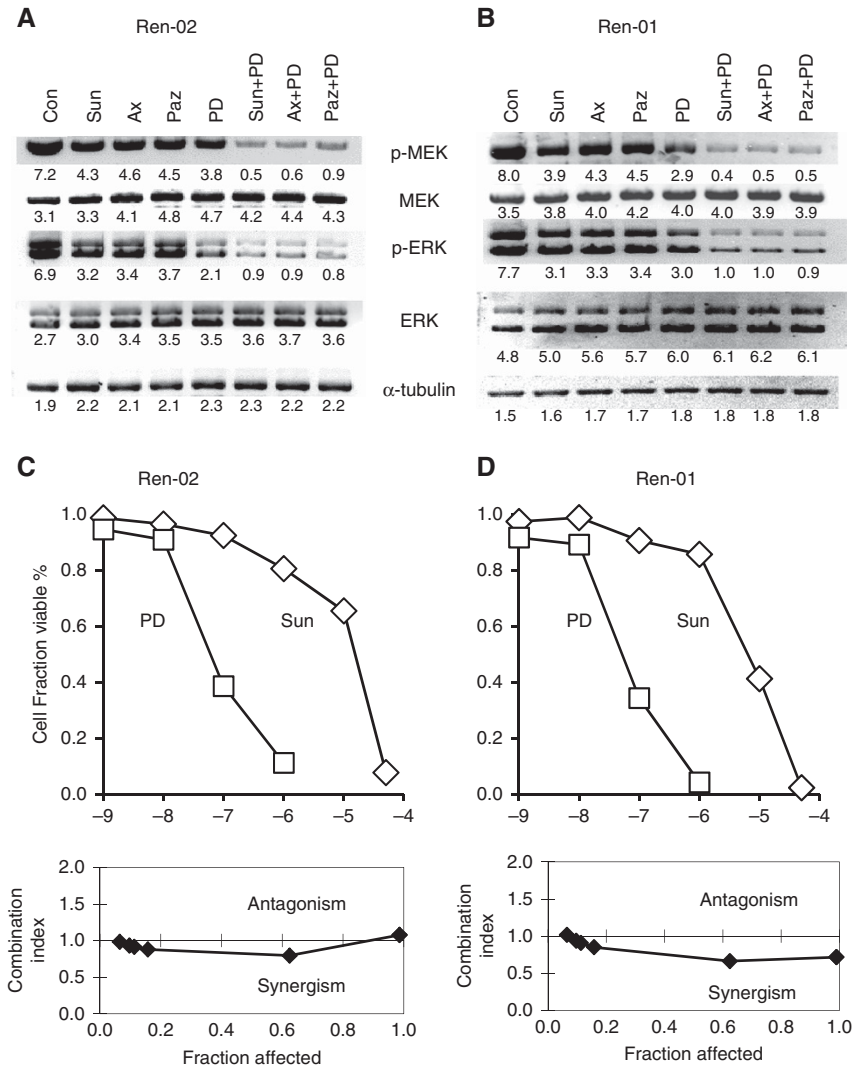

Figure 4. Immunoblot analysis of phospho-MEK1/2 and phospho-ERK1/2 in (**A**) Ren-02 RCC tumour lysates (20 μg) after long-term treatment (d62) *in vivo*. Mice received daily sunitinib (40 mg kg^{-1} p.o. q.d.), axitinib (30 mg kg^{-1} p.o. bid), pazopanib (100 mg kg^{-1} p.o. bid) and PD-0325901 (4 mg kg^{-1} p.o. q.d.). Tumours were harvested 2 h after drug dosing. (**B**) Similar analysis was performed on Ren-01 RCC cells in culture. Cells were treated for 24 h with sunitinib (2 μM), axitinib (2 μM) or pazopanib (2 μM), either alone or in combination with PD-325901 (1 nM). Numbers represent band densitometric quantisation. Sensitivity of (**C**) Ren-02 and (**D**) Ren-01 cells to sunitinib and PD-0325901 *in vitro*. Cell viability was determined following 48 h exposure to single agents or drug combinations (sunitinib: 10^{-9}–5×10^{-5} M; PD-0325901: 10^{-11}–5×10^{-7} M). Chou-Talalay analysis determined combination index (CI). CI > 1 indicates antagonism, CI = 1 indicates additivity, CI < 1 indicates synergy.

granulocytic G-MDSC were present in untreated controls and their levels were markedly increased after tumours became resistant to sunitinib, but decreased after resistance was reversed via MEK inhibition (Figure 5A). Comparing host effects of different TKI, axitinib may have reduced immunosuppressive effects compared with sunitinib (Stehle *et al*, 2013), consistent with our findings. Frequencies of infiltrating G-MDSC correlated with intra-tumoural levels of G-CSF (Figure 5B), consistent with the role of G-CSF in attracting neutrophils. Furthermore, ligation of CXCR4 and CXCR7 (both significantly induced during escape; Figure 2), also promote MAPK activation. These findings suggest that tumour-derived factors that promote G-MDSC infiltration of RCC tumours may contribute to acquired sunitinib resistance.

DISCUSSION

Development of an RCC PDX model that responds to sunitinib in a biphasic manner (response followed by escape) has revealed underlying gene expression changes in both tumour and host compartments. This biphasic tumour growth pattern occurred regardless of the likely scenario of Ren-02 cells being resistant to anti-VEGF antibody, since they were derived from a lesion that developed following bevacizumab treatment. This may reflect inhibition of other growth stimulatory pathways by TKIs and is consistent with the observation that different anti-VEGF agents demonstrate clinical activity when administered in sequence. Tumour response to sunitinib was associated with induction of apoptosis regulators, TNF signalling members, enhanced cellular movement and signalling. Tumour escape was characterised by induction of VEGFA, EPO, MEK/ERK family members, IL-8, as well as strong induction of host immune cell trafficking, inflammatory response and MDSC tumour infiltration. Combination treatment with sunitinib and a MEK inhibitor resulted in enhanced tumour suppression *in vivo*.

Enthusiasm for TKIs in treating mRCC has been tempered by the development of drug resistance. As a class, VEGF TKI (sunitinib, pazopanib and axitinib) have revolutionised mRCC management since 2005, extending progression-free survival.

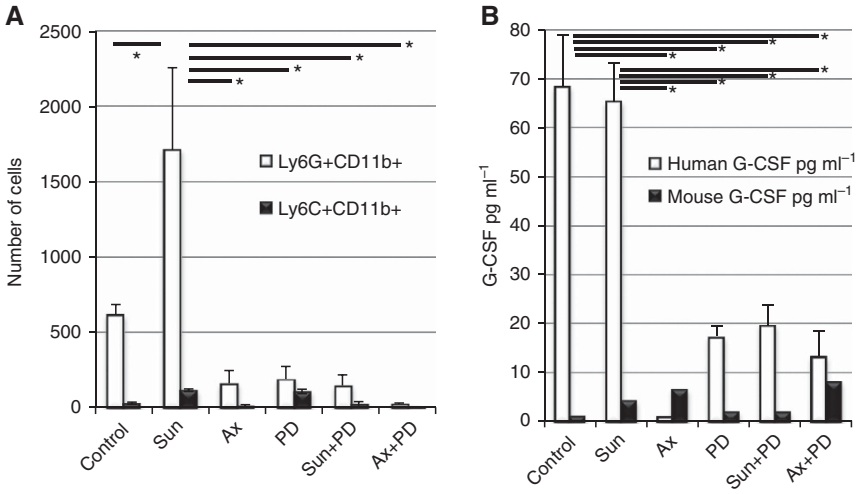

Figure 5. (A) Enumeration of infiltrating MDSC in tumours harvested after long-term (d62, mean tumour volume = 412 mm^3) treatment. After digesting tumours, cells were counted and stained with anti-CD11b PE, anti-Ly6G FITC and anti-Ly6C APC antibodies for flow cytometry analysis. The per cent Ly6G + CD11b + (G-MDSC) and Ly6C + CD11b + (M-MDSC) cells were then multiplied by the number of viable cells per tumour. Ly6G + CD11b + were present in vehicle-treated controls and their numbers were increased after tumours became resistant to sunitinib, but decreased after resistance was reversed via MEK inhibition. (**B**) Intra-tumoural G-CSF levels. Lysates from tumours were analysed by ELISA for levels of both human and murine G-CSF. Frequencies of infiltrating G-MDSC correlated with intra-tumoural levels of human G-CSF. Horizontal bars and * indicate $P<0.01$ by paired *t*-test, $n=4$.

Unfortunately, disease control is temporary and when progression occurs, sequential therapy consisting of switching to another VEGF TKI or mTOR inhibitor is the current standard of care (Escudier *et al*, 2012a, b). Selection of a VEGF TKI or an mTOR inhibitor as second-line therapy is dependent on patient-specific factors, including toxicity profile, previous response, and comorbidities.

Several preclinical models of VEGF TKI resistance have explored the relationship between resistance and the tumour microenvironment. A recent *in vivo* study demonstrated that mice implanted with RCC xenografts acquired resistance after sorafenib treatment, but could be rendered sensitive after re-implantation of the same cells into naive mice. Gene expression studies comparing profiles of untreated with re-sensitised tumours suggested that resistance to sorafenib was reversible and dependent on the tumour microenvironment (Zhang *et al*, 2011). When a sunitinib-resistant human RCC metastasis was inoculated as a xenograft, tumour regained sensitivity to sunitinib (Hammers *et al*, 2010). However, *in vitro* studies with a cell line established from the same xenograft showed that sunitinib had no direct anti-tumour effect at physiological concentrations, suggesting that escape mechanisms against VEGF TKI may be a function of the tumour microenvironment. Sunitinib-resistant xenografts of cell lines 786-O, A-498, SN12C displayed increased microvessel density and increased plasma levels of pro-angiogenic interleukin-8. Administration of neutralising IL-8 antibody restored sensitivity to sunitinib, demonstrating another potential escape mechanism from VEGF TKI therapy (Huang *et al*, 2010b).

VEGF TKI inhibit a diverse but overlapping spectrum of tyrosine kinase receptors, including VEGF-R, PDGF-R, KIT, FLTS and CSF-1R (Gotink and Verheul, 2010). The RAS/RAF/MEK/ERK signalling cascade acts downstream of TKRs such as VEGF-R, PDGF-R, c-Kit (Gotink and Verheul, 2010). Once activated, the ERK transcription factor results in expression of proteins involved in cell proliferation, angiogenesis, survival, mitosis and migration (Friday and Adjei, 2008). Activating mutations in these proteins are found pancreatic, lung, colorectal and skin cancer, and preclinical studies with MEK inhibitors offer a rationale for use in targeted therapy (Roberts and Der, 2007). In Phase I/II clinical trials, the selective MEK inhibitors PD-325901 and AZD6244 showed modest activity in advanced cancers, and remain in development as combination therapy (Rinehart *et al*, 2004; Haura *et al*, 2010).

A number of preclinical studies have demonstrated rationale for the addition of a MEK inhibitor to VEGF TKI therapy. One recent study indicates the MEK inhibitor trametinib overcomes resistance to sunitinib in an RCC PDX model (Bridgeman *et al*, 2016); this study shows the drug combination targets the vasculature and inhibits tube formation, which supports our contention that sunitinib plus MEK inhibition acts primarily via a host-mediated cellular mechanism, rather than direct anti-proliferative effects against tumour parenchymal cells. Our demonstration that the TKI/MEK inhibitor combination causes suppression of MDSC infiltration into tumours (Figure 5) likely results in decreased angiogenesis.

Mice bearing Lewis lung carcinoma tumours that were refractory to anti-VEGF antibody responded to combination therapy with a MEK inhibitor plus anti-VEGF or anti-G-CSF, which reduced tumour growth and angiogenesis (Phan *et al*, 2013). This study also showed that host myeloid cells were involved in the resistance to anti-VEGF antibody via a mechanism that was dependent on G-CSF production by the RAS/MEK/ERK pathway. Microarray analysis of genes overexpressed in the escape phase in the present study is consistent with mobilisation and activation of myeloid cells, suggesting that myeloid cells are involved in the resistance to sunitinib. In mRCC patients, high baseline neutrophil count and lack of reduction of neutrophil count during sunitinib therapy were associated with shorter progression-free survival/overall survival (Gooden *et al*, 2011; Kobayashi *et al*, 2013). Host myeloid cells were also a factor in sunitinib resistance in a RCC xenograft model that was linked to reduction in p53-dependent gene expression and appearance of the p53 antagonist, HDMX. Treating mice with the MI-319 inhibitor of HDMX plus sunitinib increased anti-tumour and anti-angiogenic activity, coinciding with a reduction in MDSC (Panka *et al*, 2013).

Our results suggest that sunitinib and axitinib differed in their impact on G-MDSC and G-CSF expression. With prolonged treatment, axitinib but not sunitinib, reduced G-MDSC numbers along with decreasing G-CSF levels in tumours, which was similar to the results with MEKi monotherapy. In this study, using a PDX model of sunitinib resistance in RCC, an unbiased whole-genome

screen has identified alternative growth pathways that were induced in the setting of sunitinib resistance. Tumours displayed decreased, yet residual phosphorylation of MEK during single agent TKI treatment, and demonstrated efficient suppression of phospho-MEK and phospho-ERK following combination TKI/MEKi therapy. This model demonstrated extension of the anti-tumour effect of sunitinib by the addition of a MEK inhibitor. Further investigation of alternative growth pathways may ultimately lead to identification of additional potential therapeutic targets.

ACKNOWLEDGEMENTS

Animal experiments using mice were performed in accordance with recommendations in Guide for the Care and Use of Laboratory Animals of the National Institutes of Health, and conducted under a protocol approved by Cleveland Clinic IACUC. These studies were supported by the Case Comprehensive Cancer Center (CCCC) Athymic Animal and Xenograft Core (DJL) and by the Translational Research and Pharmacology Core Facility (JJP) of CCCC (P30 CA43703) and an NIH grant R01CA150959 (JHF).

CONFLICT OF INTEREST

JHF received sponsored research support from Pfizer. BIR received research and consulting support from Pfizer. The remaining authors declare no conflict of interest.

REFERENCES

Beider K, Bitner H, Leiba M, Gutwein O, Koren-Michowitz M, Ostrovsky O, Abraham M, Wald H, Galun E, Peled A, Nagler A (2014) Multiple myeloma cells recruit tumor-supportive macrophages through the CXCR4/CXCL12 axis and promote their polarization toward the M2 phenotype. *Oncotarget* **5**(22): 11283–11296.

Bridgeman VL, Wan E, Foo S, Nathan MR, Welti JC, Frentzas S, Vermeulen PB, Preece N, Springer CJ, Powles T, Nathan PD, Larkin J, Gore M, Vasudev NS, Reynolds AR (2016) Preclinical evidence that trametinib enhances the response to antiangiogenic tyrosine kinase inhibitors in renal cell carcinoma. *Mol Cancer Ther* **15**(1): 172–183.

Casanovas O, Hicklin DJ, Bergers G, Hanahan D (2005) Drug resistance by evasion of antiangiogenic targeting of VEGF signaling in late-stage pancreatic islet tumors. *Cancer Cell* **8**(4): 299–309.

Cheah MT, Chen JY, Sahoo D, Contreras-Trujillo H, Volkmer AK, Scheeren FA, Volkmer JP, Weissman IL (2015) CD14-expressing cancer cells establish the inflammatory and proliferative tumor microenvironment in bladder cancer. *Proc Natl Acad Sci USA* **112**(15): 4725–4730.

Chou TC, Talalay P (1984) Quantitative analysis of dose-effect relationships: the combined effects of multiple drugs or enzyme inhibitors. *Adv Enzyme Regul* **22**: 27–55.

Escudier B, Eisen T, Porta C, Patard JJ, Khoo V, Algaba F, Mulders P, Kataja V. Group EGW (2012a) Renal cell carcinoma: ESMO Clinical Practice Guidelines for diagnosis, treatment and follow-up. *Ann Oncol* **23**(Suppl 7): vii65–vii71.

Escudier B, Szczylik C, Porta C, Gore M (2012b) Treatment selection in metastatic renal cell carcinoma: expert consensus. *Nat Rev Clin Oncol* **9**(6): 327–337.

Finke J, Ko J, Rini B, Rayman P, Ireland J, Cohen P (2011) MDSC as a mechanism of tumor escape from sunitinib mediated anti-angiogenic therapy. *Int Immunopharmacol* **11**(7): 856–861.

Fischer C, Jonckx B, Mazzone M, Zacchigna S, Loges S, Pattarini L, Chorianopoulos E, Liesenborghs L, Koch M, De Mol M, Autiero M, Wyns S, Plaisance S, Moons L, van Rooijen N, Giacca M, Stassen JM, Dewerchin M, Collen D, Carmeliet P (2007) Anti-PlGF inhibits growth of VEGF(R)-inhibitor-resistant tumors without affecting healthy vessels. *Cell* **131**(3): 463–475.

Friday BB, Adjei AA (2008) Advances in targeting the Ras/Raf/MEK/Erk mitogen-activated protein kinase cascade with MEK inhibitors for cancer therapy. *Clin Cancer Res* **14**(2): 342–346.

Gooden MJ, de Bock GH, Leffers N, Daemen T, Nijman HW (2011) The prognostic influence of tumour-infiltrating lymphocytes in cancer: a systematic review with meta-analysis. *Br J Cancer* **105**(1): 93–103.

Gotink KJ, Verheul HM (2010) Anti-angiogenic tyrosine kinase inhibitors: what is their mechanism of action? *Angiogenesis* **13**(1): 1–14.

Hammers HJ, Verheul HM, Salumbides B, Sharma R, Rudek M, Jaspers J, Shah P, Ellis L, Shen L, Paesante S, Dykema K, Furge K, Teh BT, Netto G, Pili R (2010) Reversible epithelial to mesenchymal transition and acquired resistance to sunitinib in patients with renal cell carcinoma: evidence from a xenograft study. *Mol Cancer Ther* **9**(6): 1525–1535.

Haura EB, Ricart AD, Larson TG, Stella PJ, Bazhenova L, Miller VA, Cohen RB, PD Eisenberg, Selaru P, Wilner KD, Gadgeel SM (2010) A phase II study of PD-0325901, an oral MEK inhibitor, in previously treated patients with advanced non-small cell lung cancer. *Clin Cancer Res* **16**(8): 2450–2457.

Huang D, Ding Y, Li Y, Luo WM, Zhang ZF, Snider J, Vandenbeldt K, Qian CN, Teh BT (2010a) Sunitinib acts primarily on tumor endothelium rather than tumor cells to inhibit the growth of renal cell carcinoma. *Cancer Res* **70**(3): 1053–1062.

Huang D, Ding Y, Zhou M, Rini BI, Petillo D, Qian CN, Kahnoski R, Futreal PA, Furge KA, Teh BT (2010b) Interleukin-8 mediates resistance to antiangiogenic agent sunitinib in renal cell carcinoma. *Cancer Res* **70**(3): 1063–1071.

Jousma E, Rizvi TA, Wu J, Janhofer D, Dombi E, Dunn RS, Kim MO, Masters AR, Jones DR, Cripe TP, Ratner N (2015) Preclinical assessments of the MEK inhibitor PD-0325901 in a mouse model of neurofibromatosis type 1. *Pediatr Blood Cancer* **62**(10): 1709–1716.

Ko JS, Zea AH, Rini BI, Ireland JL, Elson P, Cohen P, Golshayan A, Rayman PA, Wood L, Garcia J, Dreicer R, Bukowski R, Finke JH (2009) Sunitinib mediates reversal of myeloid-derived suppressor cell accumulation in renal cell carcinoma patients. *Clin Cancer Res* **15**(6): 2148–2157.

Kobayashi M, Kubo T, Komatsu K, Fujisaki A, Terauchi F, Natsui S, Nukui A, Kurokawa S, Morita T (2013) Changes in peripheral blood immune cells: their prognostic significance in metastatic renal cell carcinoma patients treated with molecular targeted therapy. *Med Oncol* **30**(2): 556.

Kumar V, Patel S, Tcyganov E, Gabrilovich DI (2016) The nature of myeloid-derived suppressor cells in the tumor microenvironment. *Trends Immunol* **37**(3): 208–220.

Oudard S, Elaidi RT (2012) Sequential therapy with targeted agents in patients with advanced renal cell carcinoma: optimizing patient benefit. *Cancer Treat Rev* **38**(8): 981–987.

Panka DJ, Liu Q, Geissler AK, Mier JW (2013) Effects of HDM2 antagonism on sunitinib resistance, p53 activation, SDF-1 induction, and tumor infiltration by CD11b + /Gr-1 + myeloid derived suppressor cells. *Mol Cancer* **12**: 17.

Phan VT, Wu X, Cheng JH, Sheng RX, Chung AS, Zhuang G, Tran C, Song Q, Kowanetz M, Sambrone A, Tan M, Meng YG, Jackson EL, Peale FV, Junttila MR, Ferrara N (2013) Oncogenic RAS pathway activation promotes resistance to anti-VEGF therapy through G-CSF-induced neutrophil recruitment. *Proc Natl Acad Sci USA* **110**(15): 6079–6084.

Porta C, Paglino C, Imarisio I, Ganini C, Sacchi L, Quaglini S, Giunta V, De Amici M (2013) Changes in circulating pro-angiogenic cytokines, other than VEGF, before progression to sunitinib therapy in advanced renal cell carcinoma patients. *Oncology* **84**(2): 115–122.

Raber PL, Thevenot P, Sierra R, Wyczechowska D, Halle D, Ramirez ME, Ochoa AC, Fletcher M, Velasco C, Wilk A, Reiss K, Rodriguez PC (2014) Subpopulations of myeloid-derived suppressor cells impair T cell responses through independent nitric oxide-related pathways. *Int J Cancer* **134**(12): 2853–2864.

Rinehart J, Adjei AA, Lorusso PM, Waterhouse D, Hecht JR, Natale RB, Hamid O, Varterasian M, Asbury P, Kaldjian EP, Gulyas S, Mitchell DY, Herrera R, Sebolt-Leopold JS, Meyer MB (2004) Multicenter phase II study of the oral MEK inhibitor, CI-1040, in patients with advanced non-small-cell lung, breast, colon, and pancreatic cancer. *J Clin Oncol* **22**(22): 4456–4462.

Roberts PJ, Der CJ (2007) Targeting the Raf-MEK-ERK mitogen-activated protein kinase cascade for the treatment of cancer. *Oncogene* **26**(22): 3291–3310.

Schefe JH, Lehmann KE, Buschmann IR, Unger T, Funke-Kaiser H (2006) Quantitative real-time RT-PCR data analysis: current concepts and the novel 'gene expression's CT difference' formula. *J Mol Med* **84**(11): 901–910.

Shojaei F, Lee JH, Simmons BH, Wong A, Esparza CO, Plumlee PA, Feng J, Stewart AE, Hu-Lowe DD, Christensen JG (2010) HGF/c-Met acts as an alternative angiogenic pathway in sunitinib-resistant tumors. *Cancer Res* **70**(24): 10090–10100.

Shojaei F, Wu X, Malik AK, Zhong C, Baldwin ME, Schanz S, Fuh G, Gerber HP, Ferrara N (2007a) Tumor refractoriness to anti-VEGF treatment is mediated by CD11b + Gr1 + myeloid cells. *Nat Biotechnol* **25**(8): 911–920.

Shojaei F, Wu X, Qu X, Kowanetz M, Yu L, Tan M, Meng YG, Ferrara N (2009) G-CSF-initiated myeloid cell mobilization and angiogenesis mediate tumor refractoriness to anti-VEGF therapy in mouse models. *Proc Natl Acad Sci USA* **106**(16): 6742–6747.

Shojaei F, Wu X, Zhong C, Yu L, Liang XH, Yao J, Blanchard D, Bais C, Peale FV, van Bruggen N, Ho C, Ross J, Tan M, Carano RA, Meng YG, Ferrara N (2007b) Bv8 regulates myeloid-cell-dependent tumour angiogenesis. *Nature* **450**(7171): 825–831.

Shultz LD, Lyons BL, Burzenski LM, Gott B, Chen X, Chaleff S, Kotb M, Gillies SD, King M, Mangada J, Greiner DL, Handgretinger R (2005) Human lymphoid and myeloid cell development in NOD/LtSz-scid IL2R gamma null mice engrafted with mobilized human hemopoietic stem cells. *J Immunol* **174**(10): 6477–6489.

Stehle F, Schulz K, Fahldieck C, Kalich J, Lichtenfels R, Riemann D, Seliger B (2013) Reduced immunosuppressive properties of axitinib in comparison with other tyrosine kinase inhibitors. *J Biol Chem* **288**(23): 16334–16347.

Vasudev NS, Goh V, Juttla JK, Thompson VL, Larkin JM, Gore M, Nathan PD, Reynolds AR (2013) Changes in tumour vessel density upon treatment with anti-angiogenic agents: relationship with response and resistance to therapy. *Br J Cancer* **109**(5): 1230–1242.

Welti JC, Gourlaouen M, Powles T, Kudahetti SC, Wilson P, Berney DM, Reynolds AR (2011) Fibroblast growth factor 2 regulates endothelial cell sensitivity to sunitinib. *Oncogene* **30**(10): 1183–1193.

Zhang L, Bhasin M, Schor-Bardach R, Wang X, Collins MP, Panka D, Putheti P, Signoretti S, Alsop DC, Libermann T, Atkins MB, Mier JW, Goldberg SN, Bhatt RS (2011) Resistance of renal cell carcinoma to sorafenib is mediated by potentially reversible gene expression. *PLoS One* **6**(4): e19144.

Zhou Q, Gallo JM (2010) Quantification of sunitinib in mouse plasma, brain tumor and normal brain using liquid chromatography-electrospray ionization-tandem mass spectrometry and pharmacokinetic application. *J Pharm Biomed Anal* **51**(4): 958–964.

Zhou SL, Zhou ZJ, Hu ZQ, Huang XW, Wang Z, Chen EB, Fan J, Cao Y, Dai Z, Zhou J (2016) Tumor-associated neutrophils recruit macrophages and T-regulatory cells to promote progression of hepatocellular carcinoma and resistance to sorafenib. *Gastroenterology* **150**(7): 1646–1658 e17.

Supplementary Information accompanies this paper on British Journal of Cancer website (http://www.nature.com/bjc)